Spin Textures in Strongly Coupled Electron Spin and Magnetic or Nuclear Spin Systems in Quantum Dots

Ramin M. Abolfath,[1,2,3,][*] Marek Korkusinski,[3] Thomas Brabec,[2] and Pawel Hawrylak[2,3]

[1]*School of Natural Sciences and Mathematics, University of Texas at Dallas, Richardson, Texas 75080, USA*
[2]*Physics Department, University of Ottawa, 150 Louis Pasteur, Ottawa, Ontario, K1N 6N5, Canada*
[3]*Institute for Microstructural Sciences, National Research Council of Canada, Ottawa, Ontario, K1A 0R6, Canada*

Controlling electron spins strongly coupled to magnetic and nuclear spins in solid state systems is an important challenge in the field of spintronics and quantum computation. We show here that electron droplets with no net spin in semiconductor quantum dots strongly coupled with magnetic ion or nuclear spin systems break down at low temperature and form a nontrivial antiferromagnetic spatially ordered spin texture of magnetopolarons. The spatially ordered combined electron-magnetic ion spin texture, associated with spontaneous symmetry breaking in the parity of electronic charge and spin densities and magnetization of magnetic ions, emerges from an *ab initio* density functional approach to the electronic system coupled with mean-field approximation for the magnetic or nuclear spin system. The predicted phase diagram determines the critical temperature as a function of coupling strength and identifies possible phases of the strongly coupled spin system. The prediction may arrest fluctuations in the spin system and open the way to control, manipulate, and prepare magnetic and nuclear spin ensembles in semiconductor nanostructures.

There is currently significant interest in developing quantum information storage and processing capabilities [1] using electron (*e*) and/or hole (*h*) spins strongly coupled to spins of either magnetic ions (MIs) and/or nuclear spins (NSs) in a number of solid state systems. This includes GaAs-based gated two-dimensional [2] and zero-dimensional systems [3–5], InAs self-assembled quantum dots [6–8], CdTe quantum dots [9–21], nanocrystals [22,23], NV centers in diamond [24], phosphor impurities in silicon [25], and carbon nanotubes [26].

In these systems, electron spins play either a role of qubits or are used to control MIs or NSs. For *e*-spin qubits, much effort is directed to determine the role of decoherence by NSs [4,5]. For an electron interacting with MI in diluted magnetic semiconductors [27,28], the central spin problem has been understood in terms of magnetopolarons (MPs)—a cloud of magnetization surrounding a localized *e* spin [28]. On the other hand, the interaction of many electrons in a spin singlet state with MIs/NSs, e.g., in a metal [29] or a quantum dot [14,15], induces a Ruderman-Kittel-Kasuya-Yosida (RKKY) interaction among MIs/ NSs. The question of whether spin textures could form in a strongly coupled two-dimensional electron-NS subsystem has been addressed recently by Loss *et al.* [30]. Both scenarios of MPs and RKKY interactions can be realized in semiconductor quantum dots containing MIs/NSs by changing electron or hole concentration with a gate, through modulation doping [14,15] or through deformation of quantum dot confining potential [17]. Spin singlet droplets are already employed in the initialization of coded qubits in lateral quantum dots [3] and as a component of

trions in the optical manipulation of spin in self-assembled quantum dots [7,8].

Currently, magnetic ordering in closed-shell quantum dots (QDs) doped with Mn ions is under question. In particular, recent work by Oszwałdowski *et al.* [21] suggests that closed-shell QDs doped with Mn do not allow magnetic ordering in the electronic singlet state and that magnetic ordering requires a pseudosinglet two-electron state which is neither a singlet nor a triplet. The authors came to such a conclusion because the ground state of a nonmagnetic two-electron system is a spin singlet but neglected the RKKY interaction previously discussed in Ref. [14]. Hence, a full understanding of the strongly interacting electronic singlet state with MI/NS in QDs still appears to be missing. In this Letter, we show that the closed-shell magnetic QDs strongly coupled with magnetic ions do allow magnetic ordering. The perturbative RKKY interaction among Mn ions for the closed-shell QDs, first discussed in Ref. [14], does not change the symmetry of the electronic ground state. In the present Letter, our nonperturbative approach predicts a novel broken symmetry electronic ground state with spin textures, a nontrivial form of magnetic ordering, followed by a ferromagnetic state of electrons and magnetic ions at very strong coupling. Because of the degeneracy of the spin textures under continuous rotational transformation, the magnetization of Mn and the charge and spin densities of *e*/*h* are expected to drift over time. We use an *ab initio* density functional approach to the *e* system and mean-field approximation for the MIs/NSs. We show that, beyond RKKY approximation [14], a spin singlet *e* droplet

corresponding to closed-shell quantum dots strongly couples with MIs/NSs. The e droplet breaks down and forms a nontrivial antiferromagnetic (AFM) spatially ordered spin texture of MPs at low temperature. For a very strongly coupled and weakly confined quantum dot system, this transition is followed by a transition to a ferromagnetic state. This prediction opens the way to controlling, manipulating, and preparing MI/NS ensembles in semiconductor nanostructures.

We focus here on closed-shell QDs [31] containing $N = 2, 6, 12, \ldots$ electrons in the presence of many spins of either NSs or MIs, e.g., mangan in CdTe [14,15,27,28]. We approximate many spins by a continuous magnetization [16,17] and study the strongly coupled e-MI system as a function of temperature T, electron number N, strength of e-MI exchange coupling J_{sd}, MI density n_m, and strength of confining potential ω_0. In particular, we find that, for a given confining potential, number of electrons, MI/NS density, and their coupling with electrons, there exists a critical temperature, T^*, for a two-dimensional nucleation and growth of inhomogeneous AFM spin textures with broken symmetry. Below T^* and above a critical e-MI exchange coupling strength, a spin singlet droplet and a homogeneous magnetization density break down and molecular states of MPs associated with individual e spins form. The MPs correspond to the inhomogeneous magnetic field of MIs, inducing an effective spatially varying potential, localizing electrons with spin-up in different positions from the electrons with spin-down, significantly changing electronic spin distribution. This is to be compared with closed-shell QDs with large confinement potential and with only two MIs [14,15]. Using exact diagonalization [14] of the interacting e-e and e-MI Hamiltonian, it has been shown that the RKKY coupling, a second-order effective interaction between MIs mediated by two e's with opposite spins, describes well the ground state with total magnetic moment $M_z = 0$ (AFM ordering) and $M_z = 2M$, ferromagnetic (FM) ordering, depending on the relative position of MIs in a QD, while maintaining the spin singlet electronic ground state with spin polarization $P_z = 0$. Here, M is the total spin of single MI/NS, e.g., $M = 5/2$ for Mn. A related problem has been recently studied where an analytical variational form of the two-electron wave function coupled to a large number of MIs, neither two-body singlet nor triplet, called a pseudosinglet, was introduced to describe partial quantum correlations of the coupled spin singlet MI system [21].

We use an *ab initio* density functional theory to describe the droplet of e's in a parabolic quantum dot with closed electronic shells for electron numbers $N = 2, 6, 12, \ldots$ and a mean-field approximation for the MIs/NSs system [16]. We employ spin unrestricted local density approximation (LSDA) for electrons, where the many-body Hamiltonian is replaced by the Kohn-Sham (KS) Hamiltonian, H_{KS}. In LSDA, the self-consistent KS orbitals are calculated for spin-up and down independently, without any additional symmetrization of their spatial dependence. The electrons interact with a magnetic field produced by the MIs, which in turn is determined self-consistently by the electron spin density. The electrons fill KS orbitals according to Fermi statistics at finite temperature, and the electronic correlations are taken into account via an exchange-correlation (XC) energy functional. In this approach, the self-consistent solutions form a large class of variational many-body wave functions; among them, the configuration with the lowest free energy is found. We also decompose the planar and perpendicular components of the confining potential of a single QD, as described in Refs. [16,17], and expand the electronic wave functions in terms of its planar, $\psi_{i\sigma}(\vec{r})$, and subband wave function, $\xi(z)$, and project H_{KS} onto the XY plane by integrating out $\xi(z)$, assuming that only the lowest energy subband is filled. Hence, KS orbitals, $\psi_{i\sigma}(\vec{r})$, are calculated by diagonalizing $H_{KS}\psi_{i\sigma}(\vec{r}) = \epsilon_{i\sigma}\psi_{i\sigma}(\vec{r})$, in real space. Here, $\epsilon_{i\sigma}$ are the KS eigenenergies, and $H_{KS} = \frac{-\hbar^2}{2m^*}\nabla_r^2 + V_\sigma$, with the KS effective potential denoted as $V_\sigma = V_{QD} + V_H + V_{XC}^\sigma - \frac{\sigma}{2}h_{sd}(\vec{r})$. $\hbar$ is the Planck constant, m^* is the e effective mass, $-e$ is the e charge, and $\sigma = \pm 1$ denotes spin-up ($\uparrow$) and down ($\downarrow$). V_{QD} is the planar confining potential of the QD, V_H and V_{XC}^σ are Hartree and spin-dependent exchange-correlation potentials, and $h_{sd}(\vec{r}) = J_{em} \int dz |\xi(z)|^2 B_M(Mb(\vec{r}, z)/k_B T)$. Here, $B_M(x)$ is the Brillouin function [27], k_B is the Boltzmann constant, $b(\mathbf{r}) = J_{sd}[n_\uparrow(\mathbf{r}) - n_\downarrow(\mathbf{r})]/2$ is the effective field seen by MIs, and $n_\sigma(\vec{r}) = \sum_i |\psi_{i\sigma}(\vec{r})\xi(z)|^2 f(\epsilon_{i\sigma})$. Here, $f(\epsilon) = 1/\{\exp[(\epsilon - \mu)/k_B T] + 1\}$ is the Fermi-Dirac distribution function, μ is the chemical potential, and $J_{em} = J_{sd}n_m M$ is the mean-field e-Mn or e-NS exchange coupling. J_{sd} is the local exchange coupling, FM for e-MI and AFM for e-NS or h-MI. The sign of J_{sd} affects the relative orientations of e/h spin polarization with respect to MIs/NSs. Finally, n_m denotes the MI/NS average density.

Our approximation in neglecting the spatial distribution of MIs is substantiated by experiments on colloidal nanocrystals and self-assembled QDs [22,23], showing that inhomogeneity in the distribution of Mn ions per QD, corresponding up to $\approx 5\%$ doping in typical magnetic semiconductors, can be neglected [27]. For nuclear spins in, e.g., GaAs, inhomogeneity due to different isotopes is unlikely to play an important role. Typical Mn density is much lower than the NS density; however, because the e-Mn exchange coupling is much higher than the e-NS exchange coupling, the J_{em} for both can be of the same order of magnitude. Therefore, we only present numerical results for a system of interacting e/h and MIs. For a strongly coupled e-MI system, we perform a numerical calculation for (Cd, Mn)Te, where $a_B^* = 5.29$ nm and $Ry^* = 12.8$ meV are the effective Bohr radius and Rydberg, the sd exchange coupling is $J_{sd} = 0.015$ eV nm^3, the effective mass $m^* = 0.106$, and

$\epsilon = 10.6$ [12]. We consider QDs with electronic shell spacing ω_0 in the range of 1–$3Ry^*$, width of 1 nm, and variable MI density n_m. For definiteness, we focus on the example of Mn isoelectronic impurity in CdTe, with the z component of $\vec{M}_I$ of impurity spin satisfying $M_z = -M, -M + 1, \ldots, M$ and $M = 5/2$. The direct Mn-Mn AFM coupling is negligible in the range of MI densities considered in this study.

The spatial dependence of the z component of magnetization $M_z(\vec{r})$ of Mn ions, solutions of the self-consistent LSDA equations for the coupled e-MI system, are shown in Figs. 1(a)–1(c) for the closed-shell parabolic QD corresponding to $\omega_0 = 2Ry^*$, $n_m = 0.1$ nm^{-3}, and temperature $T = 0.5$ K for $N = 2$ [Fig. 1(a)], $N = 6$ [Fig. 1(b)], and $N = 12$ [Fig. 1(c)]. Note that the total magnetization per unit area A, $\langle M_z \rangle = \frac{1}{A} \int d^2 r \langle M_z(\vec{r}) \rangle = 0$, indicates the net AFM ordering of MIs. These states clearly resemble spin textures with broken rotational symmetry. We see two spatially separated magnetization clouds for the $N = 2$
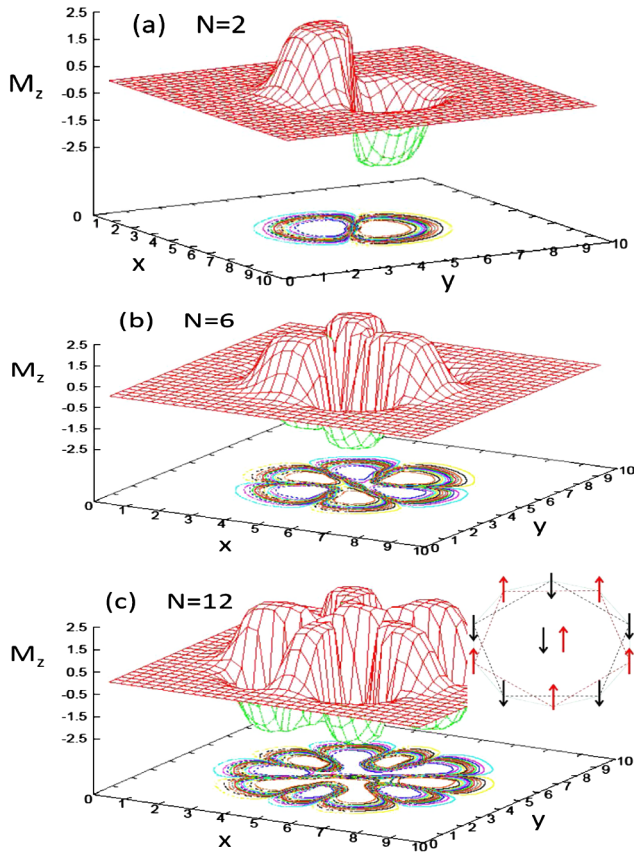

FIG. 1 (color online). The spatial profile of magnetization M_z for a closed-shell parabolic QD with $\omega_0 = 2Ry^*$ and $n_m = 0.1$ nm^{-3}. (a)–(c) correspond to $N = 2, 6, 12$ at $T = 0.5$ K and $J_{sd} = 15$ meV nm^{-3}. The coordinates (x, y) are expressed in the effective Bohr radius. The inset in Fig. 1(c) shows a decagon molecular structure of the $N = 12$ closed-shell QD with a molecular state of 12 MPs, each shown by an arrow. The directions of arrows show the direction of M_z in each MP.

quantum dot, six for $N = 6$, and 12 for $N = 12$. Hence, we consider these states as molecules of MPs. The inset shows schematically the e-spin density for 12 electrons with a decagon ring structure and two electrons in the middle in a form of a spin corral, a circular symmetric spin texture [see Fig. 1(c)]. The inhomogeneous spin density gives way to a uniform solution in which $M_z = s_z = 0$ for $T > T^* \approx 2$ K independent of N. Note that this finding is in contrast with open-shell FM states that are stable up to $T \approx 20$ K [16,17] and the FM state proposed recently in Ref. [21] for closed-shell QDs.

To investigate the origin and stability of AFM states presented in this Letter, we focus on a closed-shell QD with $N = 2$. Let us first consider the RKKY interaction between two MIs in a QD [14] with $N = 2$ at positions $\vec{R}_1 = (X, 0)$ and $\vec{R}_2 = (-X, 0)$: $J(X) = -\gamma(2 - 5X^2)e^{-X^2}$ is the e-mediated effective interaction between two MIs, where $\gamma = (J^{2D}/\pi l_0)^2 [1/(16\omega_0)]$, and the distance is measured in $l_0 = \sqrt{\hbar/(2m^*\omega_0)}$. Here, $J^{2D} = J_{sd}2/d$ and d is the thickness of the QD in the perpendicular direction [14]. We see that for $X > \sqrt{2/5}$ the interaction is AFM. It is now possible to imagine that the RKKY interaction triggers a broken symmetry state where the exchange interaction localizes an electron with spin-up on the left MI and a spin-down electron on the right MI, a two-atomic molecule of MP, seen in Fig. 1(a). In Fig. 2, we show self-consistent solutions of LSDA equations, including the effective potential V_σ and the spatial profile of spin-dependent KS wave functions for the parabolic confining potential with level spacing $\omega_0 = 2Ry^*$. In Fig. 2(a), $T = 2$ K and the paramagnetic state with $M_z = P_z = 0$ is the ground state. The spin-dependent effective potential V_σ is shown with open circles in which $V_\uparrow = V_\downarrow$. In this case, we find that the self-consistent KS eigenenergies and eigenstates with opposite spins are identical, $\epsilon_{0\uparrow} = \epsilon_{0\downarrow}$ and $\psi_{0\uparrow} = \psi_{0\downarrow}$. In Fig. 2(b), we present our results for $T = 0.5$ K. Interestingly, with decreasing temperature, a continuous displacement in spin-dependent wave functions develops that spontaneously breaks the circular symmetry of the QD, as discussed above. In this case, we find two degenerate spatially separated wave functions $\psi_{0\uparrow}$ and $\psi_{0\downarrow}$, with $\epsilon_{0\uparrow} = \epsilon_{0\downarrow}$. These are analogues to the nucleation of the para-H$_2$ molecule from para-He if two nuclei of He undergo a continuous fragmentation. A two-dimensional profile of e-spin polarization $P_z = (n_\uparrow - n_\downarrow)/2$, shown in (c), is also a result of the spontaneous spatial spin separation of KS orbitals. Two asymmetric bumps observed in effective potentials $V_\uparrow$ and $V_\downarrow$ are the result of the spontaneous formation of AFM spin texture in M_z, shown explicitly in Fig. 1.

The spontaneous symmetry breaking and the formation of MPs depend on the parameters of the system. For example, in the example studied here, the critical temperature depends on the e-MI exchange coupling strength $J_{em} = J_{sd}n_m M$, which is proportional to exchange
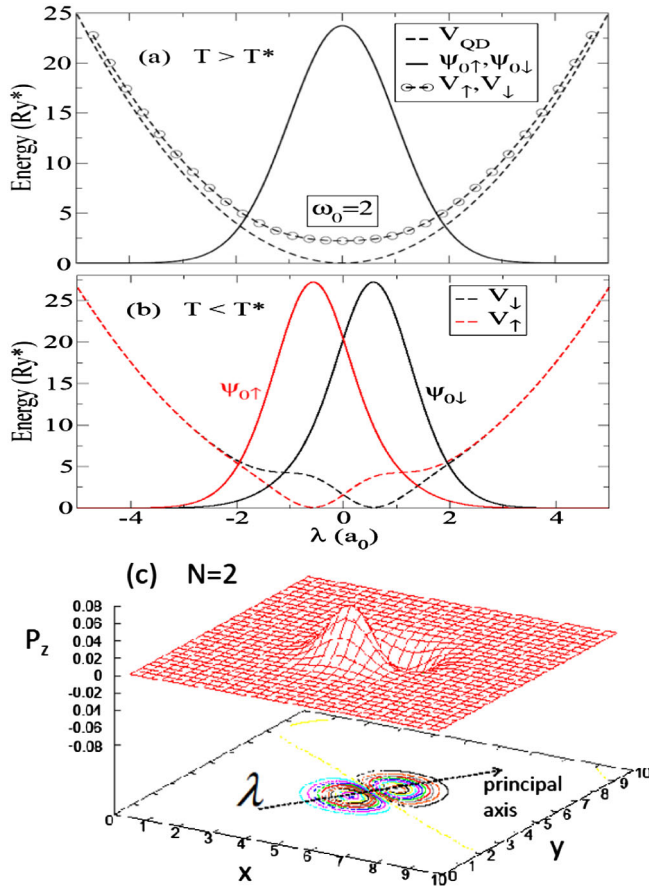
FIG. 2 (color online). The spatial dependence of wave functions $\psi_{0\uparrow}$ and $\psi_{0\downarrow}$, effective potentials, and P_z in a QD with $N = 2$, $\omega_0 = 2Ry^*$, and $n_m = 0.1$ nm^{-3}. In (a), $T > T^*$, $M_z = P_z = 0$, and $\psi_{0\uparrow} = \psi_{0\downarrow}$. The dashed lines show the QD parabolic confining potential, V_{QD}. The spin-dependent effective potential $V_\sigma = V_{QD} + V_H + V_{XC}^\sigma - \sigma h_{sd}/2$ is shown by dashed lines with open circles, with $V_\uparrow = V_\downarrow$. In (b), $T < T^*$. A pronounced separation of spin-up and down wave functions and two asymmetric bumps in $V_\uparrow$ and $V_\downarrow$ are shown. In (b), the bottoms of potentials $V_\uparrow$ and $V_\downarrow$ are shifted to zero. The horizontal axis used in (a) and (b) is plotted along the diagonal direction of P_z, shown as the principal axis by a dashed arrow in (c) and denoted by λ in (b). The planar coordinates (x, y) are expressed in the effective Bohr radius (a_0).
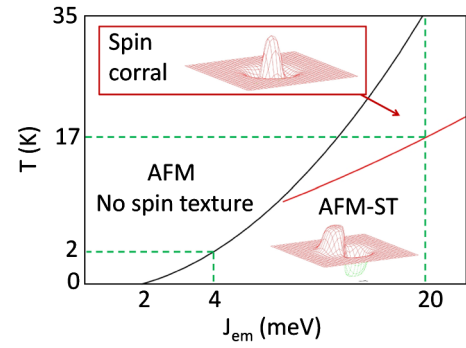

FIG. 3 (color online). Spin texture (ST) phase diagram, temperature T vs e-MI coupling strength J_{em} of the $N = 2$ closed-shell QD with $\omega_0 = 2Ry^*$.

h-MI exchange coupling, and $n_m = 0.1$ nm^{-3}, we find $T_1^* = 17$ and $T_2^* = 35$ K. We emphasize that the total spin of electrons is zero for the range of parameters considered in this study. However, by increasing J_{em} above a critical value that is determined by the energy difference in the lowest unoccupied and highest occupied KS energy levels, a transition to the spin triplet takes place [16,17,19]. For the typical quantum dots investigated here, the critical value of $J_{em}^* \approx 30$ meV is much higher than the range of exchange couplings J_{em} responsible for the spin textures predicted here.

To summarize, low temperature solutions of the *ab initio* density functional approach to electrons in closed-shell quantum dots strongly coupled with the magnetic and/or nuclear spins described in the mean-field approximation show the existence of a broken symmetry spatially inhomogeneous state of geometrically ordered molecules of magnetopolarons. The phase diagram of topologically stable nontrivial AFM states determined by the number N of electrons in a quantum dot, MI density, exchange coupling strength, temperature, and confining potential is predicted. The predicted ordered spin states may arrest fluctuations in the spin system and open the way to control, manipulate, and prepare MI/NS ensembles in semiconductor nanostructures for quantum information processing and storage.

coupling, MI density, and MI spin. Figure 3 shows the phase diagram of the $N = 2$ closed-shell QD with $\omega_0 = 2Ry^*$ and $n_m = 0.1$ nm^{-3}. The curves show the critical temperature as a function of J_{em}. In the limit of low J_{em}, e.g., either for e and/or low density of MIs, a direct transition from the AFM spin texture, shown in the inset, to the normal state is seen. For high J_{em}, e.g., for either h and/or high density of MIs, a transition through an intermediate state of spin corral, shown in the inset (see Fig. 3), is observed. This is a transition from the rotational symmetry breaking state, stable at low temperatures, to another type of spin texture with rotational symmetry, stable within $T_1^* \le T \le T_2^*$. For $J_{sd} = 75$ meV nm^3, corresponding to

*Present address: Department of Therapeutic Radiology, Yale School of Medicine, Yale University, New Haven, CT 06520, USA.

[1] *Semiconductor Quantum Bits*, edited by O. Benson and F. Henneberger (World Scientific, Singapore, 2008).

[2] G. Yusa, K. Muraki, K. Takashina, K. Hashimoto, and Y. Hirayama, Nature (London) **434**, 1001 (2005).

 [3] J. R. Petta, A. C. Johnson, J. M. Taylor, E. A. Laird, A. Yacoby, M. D. Lukin, C. M. Marcus, M. P. Hanson, and A. C. Gossard, Science **309**, 2180 (2005).

 [4] D. J. Reilly, J. M. Taylor, J. R. Petta, C. M. Marcus, M. P. Hanson, and A. C. Gossard, Phys. Rev. Lett. **104**, 236802 (2010).

 [5] O. Tsyplyatyev and D. Loss, Phys. Rev. Lett. **106**, 106803 (2011); A. V. Khaetskii, D. Loss, and L. Glazman, *ibid.* **88**, 186802 (2002); R. de Sousa and S. Das Sarma, Phys. Rev. B **67**, 033301 (2003); W. Yao, R.-B. Liu, and L. J. Sham, *ibid.* **74**, 195301 (2006); G. Chen, D. L. Bergman, and L. Balents, *ibid.* **76**, 045312 (2007).

 [6] G. Kioseoglou, M. Yasar, C. H. Li, M. Korkusinski, M. Diaz-Avila, A. T. Hanbicki, P. Hawrylak, A. Petrou, and B. T. Jonker, Phys. Rev. Lett. **101**, 227203 (2008).

 [7] M. N. Makhonin, K. V. Kavokin, P. Senellart, A. Lemaître, A. J. Ramsay, M. S. Skolnick, and A. I. Tartakovskii, Nature Mater. **10**, 844 (2011).

 [8] E. Baudin, E. Benjamin, A. Lemaître, and O. Krebs, Phys. Rev. Lett. **107**, 197402 (2011).

 [9] L. Besombes, Y. Léger, L. Maingault, D. Ferrand, and H. Mariette, Phys. Rev. Lett. **93**, 207403 (2004).

[10] J. Fernández-Rossier and L. Brey, Phys. Rev. Lett. **93**, 117201 (2004).

[11] A. O. Govorov, Phys. Rev. B **72**, 075358 (2005).

[12] F. Qu and P. Hawrylak, Phys. Rev. Lett. **95**, 217206 (2005).

[13] Y. Léger, L. Besombes, L. Maingault, D. Ferrand, and H. Mariette, Phys. Rev. Lett. **95**, 047403 (2005); Y. Léger, L. Besombes, J. Fernández-Rossier, L. Maingault, and H. Mariette, *ibid.* **97**, 107401 (2006).

[14] F. Qu and P. Hawrylak, Phys. Rev. Lett. **96**, 157201 (2006).

[15] S.-J. Cheng and P. Hawrylak, Europhys. Lett. **81**, 37 005 (2008).

[16] R. M. Abolfath, P. Hawrylak, and I. Žutić, Phys. Rev. Lett. **98**, 207203 (2007); New J. Phys. **9**, 353 (2007).

[17] R. M. Abolfath, A. G. Petukhov, and I. Žutić, Phys. Rev. Lett. **101**, 207202 (2008).

[18] C. Le Gall, L. Besombes, H. Boukari, R. Kolodka, J. Cibert, and H. Mariette, Phys. Rev. Lett. **102**, 127402 (2009).

[19] Nga T. T. Nguyen and F. M. Peeters, Phys. Rev. B **78**, 045321 (2008); **80**, 115335 (2009).

[20] A. H. Trojnar, M. Korkusiński, E. S. Kadantsev, P. Hawrylak, M. Goryca, T. Kazimierczuk, P. Kossacki, P. Wojnar, and M. Potemski, Phys. Rev. Lett. **107**, 207403 (2011).

[21] R. Oszwałdowski, I. Žutić, and A. G. Petukhov, Phys. Rev. Lett. **106**, 177201 (2011).

[22] S. T. Ochsenbein, Y. Feng, K. M. Whitaker, E. Badaeva, W. K. Liu, X. Li, and D. R. Gamelin, Nature Nanotech. **4**, 681 (2009); R. Beaulac, Y. Feng, J. W. May, E. Badaeva, D. R. Gamelin, and X. Li, Phys. Rev. B **84**, 195324 (2011); K. M. Whitaker *et al.*, Nano Lett. **11**, 3355 (2011).

[23] R. Viswanatha, J. M. Pietryga, V. I. Klimov, and S. A. Crooker, Phys. Rev. Lett. **107**, 067402 (2011).

[24] G. D. Fuchs, G. Burkard, P. V. Klimov, and D. D. Awschalom, Nature Phys. **7**, 789 (2011).

[25] B. E. Kane, Nature (London) **393**, 133 (1998).

[26] H. O. H. Churchill, A. J. Bestwick, J. W. Harlow, F. Kuemmeth, D. Marcos, C. H. Stwertka, S. K. Watson, and C. M. Marcus, Nature Phys. **5**, 321 (2009).

[27] J. K. Furdyna, J. Appl. Phys. **64**, R29 (1988); T. Dietl, H. Ohno, and F. Matsukura, Phys. Rev. B **63**, 195205 (2001); M. Abolfath, T. Jungwirth, J. Brum, and A. H. MacDonald, *ibid.* **63**, 054418 (2001).

[28] *The Physics of Diluted Magnetic Semiconductors*, Springer Series in Materials Science, edited by J. Gaj and J. Kossut (Springer-Verlag, Berlin, 2011).

[29] M. A. Ruderman and C. Kittel, Phys. Rev. **96**, 99 (1954); T. Kasuya, Prog. Theor. Phys. **16**, 45 (1956); K. Yosida, Phys. Rev. **106**, 893 (1957).

[30] D. Loss, F. L. Pedrocchi, and A. J. Leggett, Phys. Rev. Lett. **107**, 107201 (2011).

[31] S. Raymond *et al.*, Phys. Rev. Lett. **92**, 187402 (2004).